

Direct imaging of surface states hidden in the third layer of Si (111)-7 × 7 surface by p_z-wave tip

Jing Wang, Lai Jin, Hua Zhou, Huixia Fu, Chuangye Song, Sheng Meng, and Jinxing Zhang

Citation: *Appl. Phys. Lett.* **113**, 031604 (2018); doi: 10.1063/1.5038954

View online: <https://doi.org/10.1063/1.5038954>

View Table of Contents: <http://aip.scitation.org/toc/apl/113/3>

Published by the [American Institute of Physics](#)

Articles you may be interested in

[Impact of the degree of Cu–Zn order in Cu₂ZnSn\(S,Se\)₄ solar cell absorbers on defect states and band tails](#)

Applied Physics Letters **113**, 033901 (2018); 10.1063/1.5036622

[Automated tuning of inter-dot tunnel coupling in double quantum dots](#)

Applied Physics Letters **113**, 033101 (2018); 10.1063/1.5031034

[Selective activation of localized mechanical resonators via a phonon waveguide](#)

Applied Physics Letters **113**, 043104 (2018); 10.1063/1.5037484

[Foreshadowing elastic instabilities by negative group velocity in soft composites](#)

Applied Physics Letters **113**, 031901 (2018); 10.1063/1.5042077

[Exclusion of injection efficiency as the primary cause of efficiency droop in semipolar \(20 \$\bar{2}\$ 1\) InGaN/GaN light-emitting diodes](#)

Applied Physics Letters **113**, 031101 (2018); 10.1063/1.5036761

[Stress mapping of a strain superlattice using scanning moiré fringe imaging](#)

Applied Physics Letters **113**, 031905 (2018); 10.1063/1.5022842

AIP | Conference Proceedings

Get **30% off** all
print proceedings!

Enter Promotion Code **PDF30** at checkout



Direct imaging of surface states hidden in the third layer of Si (111)-7 × 7 surface by p_z -wave tip

Jing Wang,^{1,a)} Lai Jin,^{1,a)} Hua Zhou,¹ Huixia Fu,² Chuangye Song,¹ Sheng Meng,^{2,b)} and Jinxing Zhang^{1,b)}

¹Department of Physics, Beijing Normal University, 100875 Beijing, China

²Institute of Physics, Chinese Academy of Science, 100190 Beijing, China

(Received 7 May 2018; accepted 28 June 2018; published online 17 July 2018)

The direct visualization of the surface states of dimers in Si (111)-7 × 7 is still challenging although the DAS model has been proposed 33 years ago. In this letter, based on the partial density of states of the atoms in the reconstructed layers examined by the first principles calculations, scanning tunneling spectroscopy images with a p_z -wave tip were carried out, which show a skull pattern at ~0.7 eV, and 9 bright short lines at ~1.00 eV in each unit cell, exhibiting obviously the electronic states from the third-layer atoms and dimers. The improved sensitivity (intensity and resolution) of scanning tunneling spectroscopy was ascribed to the enhanced tunneling matrix elements for p_z -wave tip compared with s-wave tip. This discovery provides us a platform to explore the quantum states hidden in the deep of the materials surface. *Published by AIP Publishing.*

<https://doi.org/10.1063/1.5038954>

Scaling of silicon (Si)-based semiconductor devices down to an atomic level has become an inevitable trend due to the increasing requirement of high density and low energy consumption in electronic devices. Thus, surface states of semiconductors become more important, which not only host the emergence of quantum phenomena,¹ but also play an important role in the functionality of shrinking electronic devices.² Si (111) surface is critical in designing electronic devices due to its 6- or 3-fold symmetry, which is well compatible with other semiconductors (e.g., GaN³), two-dimensional (2D) materials (e.g., MoS₂⁴ and graphene⁵), and topological insulators (e.g., Bi₃Se₂⁶). Si (111)-7 × 7 surface with the lowest surface energy^{7,8} and intriguing structure has aroused general interests.^{1,2,7,8} In such a surface, dimers, among many aggregation structures of Si-based surfaces, are critical for altering surface symmetry,⁹ forming self-ordered 1D chain structures¹⁰ and thus having a strong impact on surface states.⁹⁻¹¹

About 60 years ago, Schlier and Farnsworth first reported Si (111)-7 × 7 surface by the employment of low-energy electron diffraction.¹² Later, Rowe and Ibach observed distinct surface states on this surface by ultraviolet photoelectron spectroscopy.¹³ In 1985, the dimer-adatom-stacking-fault (DAS) model¹⁴ for Si (111)-7 × 7 surface was first proposed, which consists of three reconstructed layers, including the main features of 12 adatoms (first layer), 6 rest atoms (second layer), 9 dimers (third layer), and one corner hole in each unit cell, as well as the stacking fault between the second and third layer in half unit cell. Each adatom, rest atom, and corner hole exhibits one dangling bond. Benefiting from the development of scanning probe technique, the atomic and electronic structures of adatoms were easily achieved by scanning tunneling microscopy (STM) due to the dangling-bond surface states. While for rest atoms, due

to the exponentially attenuated tunneling current (I_t) with the increasing space between the tip and the topmost atomic layer,¹⁵ it becomes much more challenging to explore them by STM only if engineering the tip radius.¹⁶ Scanning tunneling spectroscopy (STS), e.g., the differential conductance spectra (dI/dV - V), however, can be used to explore the rest atoms by selectively picking up the dangling bond states at specific energy levels while suppressing the counterpart of adatoms. Therefore, STS provides us a potential technique to explore the deeper electronic information hidden under the surface. Nevertheless, due to the limited sensitivity (intensity and resolution) of STS in depth, to date, it is still a big challenge to direct visualize the dimers hidden in the “third layer” of Si (111)-7 × 7 surface.

In Bardeen's pioneering work:¹⁵ $\frac{dI}{dV} \approx \frac{2e^2}{h} \rho_{tip}(E_F + \varepsilon) \rho_{sample}(E_F - eV + \varepsilon) |M(\varepsilon)|^2$, where $\rho_{tip}(E_F + \varepsilon)$ and $\rho_{sample}(E_F - eV + \varepsilon)$ represent the local density of states (LDOSs) of tip and sample, respectively, and $|M(\varepsilon)|^2 \propto \exp(-2d\sqrt{\frac{2m}{\hbar^2}(\frac{\Phi_{tip} + \Phi_{sample}}{2} + \frac{eV}{2} - \varepsilon)})$ describes the transmission factor, which is related to wave functions of the tip apex and sample surface. While in Tersoff-Hamann approximation,^{17,18} due to an s-wave tip was assumed, the LDOSs of the tip and the transmission factor ($|M(\varepsilon)|^2$) are considered to be voltage independent. Hence, the dI/dV is proportional to the LDOSs of the sample at the tip position: $\frac{dI}{dV} \propto \rho_{sample}(r_0, E_F)$,¹⁵ where r_0 describes the distance between the center of the point-like tip and the topmost surface, and E_F indicates the Fermi energy of the sample. Later, Chen developed the derivative rule¹⁹ based on Bardeen's theory, where $M(\varepsilon)$ is proportional to the linear combination of spatial derivatives of single-electron wave functions of the sample surface, which indicates an enhanced transmission factor of $1 + q^2/\kappa^2$ and $[1 + (3q^2/2\kappa^2)]^2$ for p_z - and d_{z^2} -wave tip compared with s-wave tip.²⁰ In addition, Ohnishi and Tsukada, also theoretically illustrated that the

^{a)}J. Wang and L. Jin contributed equally to this work.

^{b)}Electronic addresses: smeng@iphy.ac.cn and jxzhang@bnu.edu.cn

tunneling current is primarily generated by the d_{z^2} dangling-bond tip state if there forms W_4 or W_5 clusters at the tip apex.²¹ Experimentally, numerous molecular orbitals^{15,22–25} were observed by altering the wave functions of tip apex by chemical decoration, which improved the sensitivity of the STS.¹⁹ Therefore, it will provide us a potential platform to explore the electronic structures of buried layers by STS technique with p - or d -wave tip state by tip-apex decoration.

In this work, the partial density of states (PDOSs) of the atoms in the Si (111)- 7×7 surface were first examined by first principles calculations. The results show that the PDOSs of the third-layer atoms and dimers predominate at the energy level of ~ 0.7 and ~ 1.0 eV, respectively, while that of the adatoms and rest atoms suppressed. Based on these results, STS images with a p_z -wave tip were carried out, which show a skull pattern at ~ 0.7 eV, and 9 bright short lines at ~ 1.0 eV in each unit cell, exhibiting obviously the electronic states from third-layer atoms and dimers. These unprecedented surface states arising from the buried layers at certain bias voltages bringing precise commensuration with DAS model after thirty years. Our observations first demonstrate experimentally the LDOSs from the third-layer atoms of Si (111)- 7×7 surface using high-oriented p_z -wave tip, which is highly matched with the surface wave functions of the sample. This work further provides us a technique to explore the deep information of other model systems such as MX_2 topological insulators or superconductors with sandwich structures.

Our STM/STS experiments were performed at 78 K. The detailed experimental and calculated conditions can be seen in the [supplementary material](#). Figure 1(a) displays the DAS model of the 2×2 supercell of Si (111)- 7×7 surface, which consists of three layers indicated by gray, blue and green transparent shadows, respectively. The blue, pink,

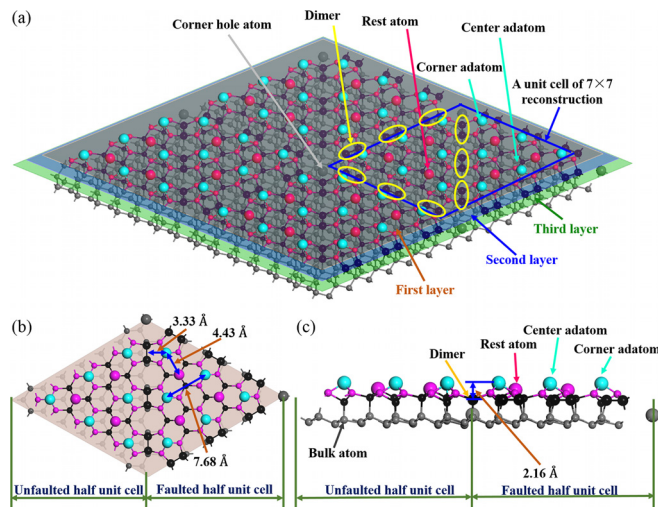


FIG. 1. 3D schematic of the DAS model for Si (111)- 7×7 surface. (a) Top-view schematics of the 2×2 supercell of the DAS model. Gray, blue and green shadow represent first, second and third lattice planes. Solid dots represent Si atoms. One (7×7) unit cell has been outlined by blue rhombus. Around the perimeter and separating the two halves are 9 dimers (yellow ellipses) lying two layers below the top surface. The pink balls denote 6 rest atoms and the reconstruction is terminated by 12 adatoms (blue balls). The gray balls indicate the bulk Si atoms. (b) and (c) The corresponding top- and side-view structure of one unit cell, respectively, labeled with lateral and vertical distance between the featured atoms.

black spheres describe the atomic arrangement of the top three layers from top to bottom, respectively and the gray spheres indicate the bulk atoms. One (7×7) unit cell has been outlined by blue rhombus. To give a distinct description, the key features including adatoms and rest atoms were indicated by the largest spheres, which exhibit one dangling bond within each atom.¹⁴ Furthermore, the key feature of dimers is highlighted by yellow ellipses. A high-resolution STM image ($V = +2$ V, $I_t = 0.3$ nA) of the reconstructed top surface can be seen in Fig. S1.¹⁶ The corresponding top- and side-view structure of one unit cell can be seen in Figs. 1(b) and 1(c) labeled with lateral and vertical distances between the featured atoms, respectively. Noting that the vertical distance (d) between dimers and adatoms is approximately 2.1 \AA ,⁸ thus conventionally, the tunneling barrier for dimers is sharply increased, causing an undetectable tunneling current as $I \propto e^{-2kd}$ in simplicity, where $k = \sqrt{2m\phi}/\hbar$.²⁶

In order to explore the possible way to resolve the effect of dimers on the electronic properties of the Si (111)- 7×7 surface, the projected density of states (PDOSs) of different types of atoms in the top three layers were calculated by the density function theory (DFT), as shown in Fig. 2(a). The black shadow and hollow parts enclosed by the curves describe the corresponding occupied and empty states of the top three-layer atoms [see the atomic models in Figs. 2(b)–2(d)], respectively. The yellow line indicates the E_F of Si (111)- 7×7 surface. The PDOSs curves for the adatoms and rest atoms show strong peaks at $\sim +0.3$ eV and ~ -0.5 eV [blue and pink arrows in Fig. 2(a)], respectively, which can be further demonstrated by the higher electron conductance (black arrows) in the DFT calculations [Fig. 2(e)]

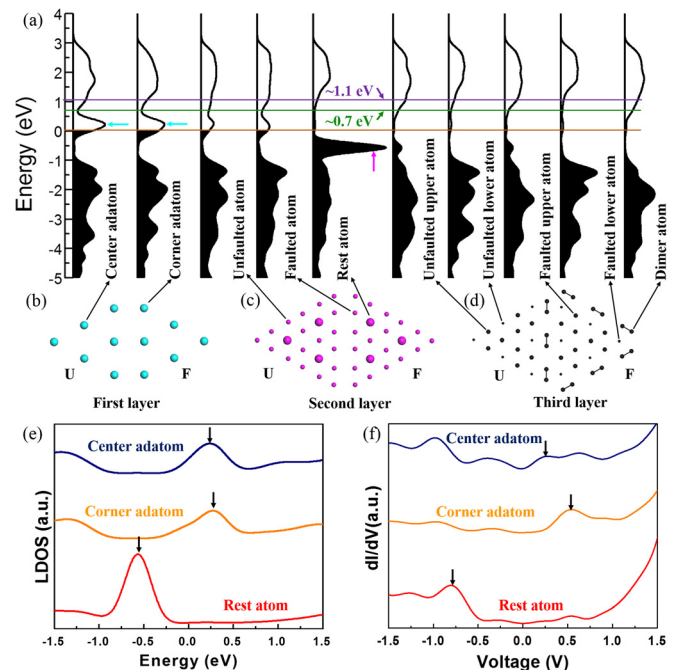


FIG. 2. First principles calculations and STSs for the DOSs localized around atoms in the reconstructed layers. (a) Calculated DOSs projected in specific atoms of the reconstructed surface. The yellow line indicates the E_F . (b)–(d) Atomic models of the corresponding first, second and third layers, highlighting the features of the center and corner adatoms (b), rest atoms (c), and dimers (d), respectively. (e) First principles calculations and (f) STSs evidence of DOSs localized around adatoms and rest atoms.

and also the experimental STS spectra [Fig. 2(f)]. Our experimental observation in Fig. 2(f) is also consistent with the previous reports.²⁷ Nevertheless, the relative intensity of PDOSs for the third-layer atoms at these specific energy levels are extreme small and thus undetectable.

Taking advantages of the functionalized tip on the spatial and energy resolutions, we deliberately modified the metal (Pt-Ir) tip with silicon atoms. Based on the above discussion, it is reasonable to vary the wave function of the tip by the modification of tip apex. For example, Si cluster decoration alters the tip state from *s*-wave to *p*-wave,²⁸ as illustrated by the color transparent shadows in the schematics of Figs. 3(a) and 3(b). The detailed process can be found in the previous reports²⁹ and Fig. S2. Figures 3(c) and 3(d) show the STM images with Pt-Ir tip and Si-decorated tip at the bias voltage of -1.5 V, respectively. From the line scanning across the long-diagonal direction in the unit cell, the rest atoms in the layer beneath the top surface can be clearly illustrated by employing functionalized tip [green curve in Fig. 3(e)] compared with the bare metal tip [blue curve in Fig. 3(e)]. Figure 3(f) describes the corresponding atomic model of adatoms and rest atoms. Figures 3(g) and 3(h) show the STS images obtained at the bias voltage of -0.7 V, which corresponds to the characteristic bias voltage for the rest atoms according to the DFT calculations [Fig. 2(e)] and our dI/dV curves [Fig. 2(f)]. The intensity of the local differential conductance increases when the functionalized tip [green curve in Fig. 3(i)] was employed compared with the bare metal tip [blue curve in Fig. 3(i)]. Figure 3(j) displays the atomic model of the second layer of Si (111) 7×7 surface. All these observations demonstrated that the modification of the tip apex with Si cluster will effectively enhance the sensitivity of the STS, which is consistent with

Chen's derivative rule, where an enhanced corrugation amplitude factor of 2.7 for p_z tip state compared with *s* tip state.²⁰ The corresponding comparison of the corrugation amplitude of different tip and sample states can be seen in the [supplementary material](#).

According to the above discussions regarding to the higher sensitivity of the decorated tip, we now try to distinct the PDOSs of multiple kinds of atoms of the reconstructed three-layer, especially the third-layer dimers, by exploring the STS images at higher energy levels (~ 1 eV). As shown in Figs. 4(a) and 4(b), a skull pattern was observed in STS image at the bias voltage of 1.09 V. The white and blue triangles of the STS image in Fig. 4(b) represent unfaulted and faulted half unit cell, respectively, indicating the stronger intensity of LDOS for the former counterpart. Compared with Figs. 3(d) and 3(h), this result implies that the electronic state of Si (111)- 7×7 surface at the bias voltage of 1.09 V arises from the reconstructed structures in addition to adatoms and rest atoms. This conclusion can be further verified by the DFT calculations [Fig. 2(a)]. The relative strength of LDOS near 1.1 eV for center and corner adatoms, second-layer atoms without dangling bond, third-layer upper atoms and dimers at the unfaulted half unit cell are 0.16, 0.11, 0.11, 0.14, and 0.15, respectively. Therefore, the brightness of STS image at the site of center is stronger than that at the site of corner, forming triangle consisted of three short edges. Besides, the intensity of LDOSs at this energy level for the third-layer upper atoms and dimer is large, indicating that STS image at the bias voltage should contain information of these atoms. In fact, these STS images [Figs. 4(a) and 4(b)] are very similar to the simulation results from Paz and Soler with a bias voltage of about $+1.0$ V.³⁰

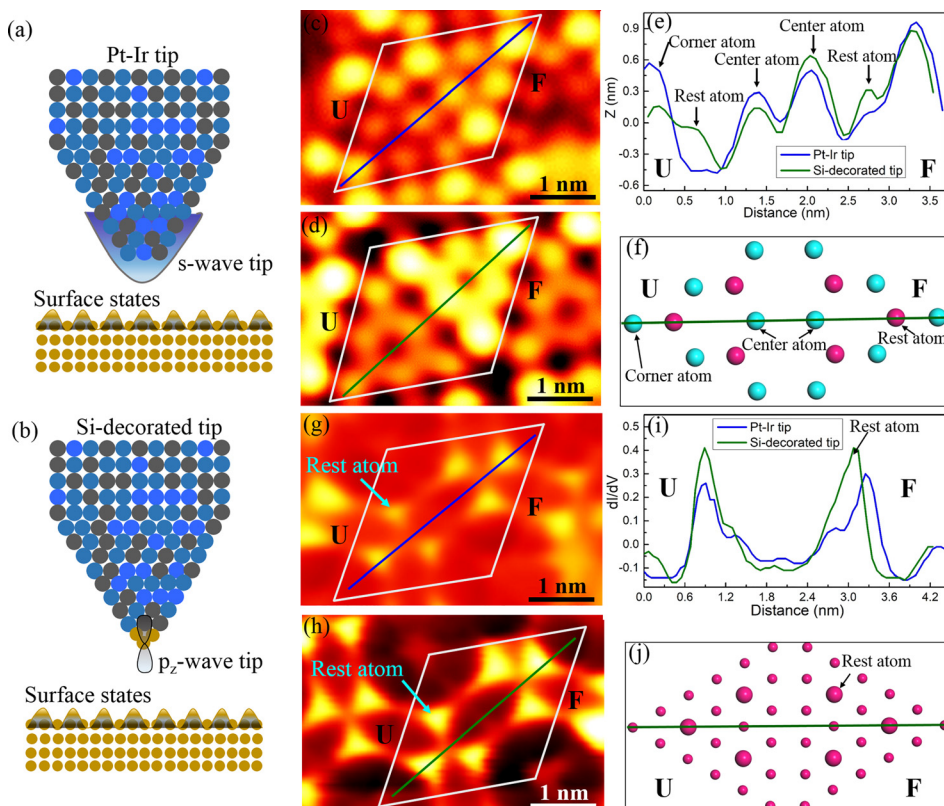


FIG. 3. Experimental evidence for the enhanced sensitivity of STM/STS with the Si-decorated Pt-Ir tip. (a) Schematics of Pt-Ir tip with *s* wave, as labeled by circular shape, and (b) Si-decorated tip with p_z wave, as labeled by the dumbbell shape. STM (c) and (d) and STS (g) and (h) images obtained with the *s*-wave (c) and (g) and p_z -wave (d) and (h) tip, respectively. The unfaulted/faulted half unit cell is labeled as “U”/“F”. The line profiles across the long diagonal of the unit cell in STM/STS images stress the refined characteristics with the assistance of Si-modified tip (d) and (h) compared to the bare Pt-Ir one (c) and (g). (e)–(j) Line scanning and atomic models according to the STM (c) and (d) and STS (g) and (h) images. Blue and pink solid dots in (f) represent adatoms and rest atoms, respectively. In (j), larger and smaller pink solid dots denote rest atoms and other atoms at the second layer, respectively.

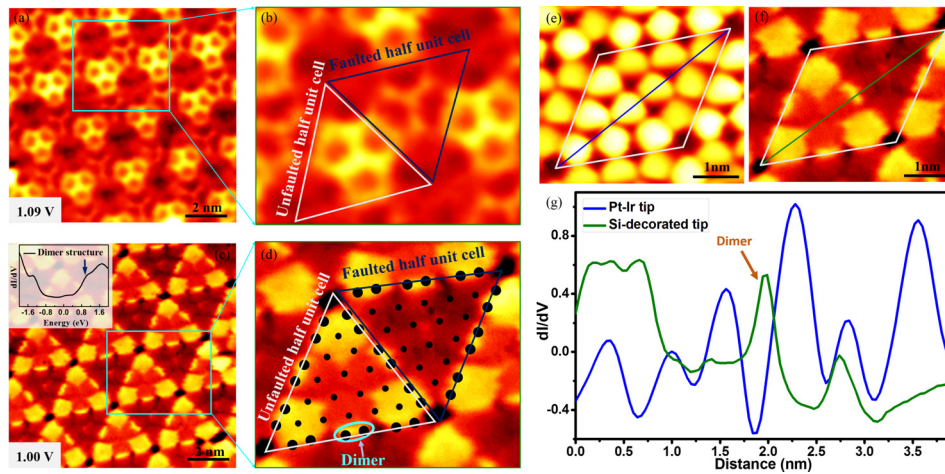


FIG. 4. STS evidence for dimers in DAS model. (a) STS image with a skull pattern at the bias voltage of 1.09 V. (b) The corresponding amplified image of the area labeled by the blue box in (a). White and blue triangles represent unfaulted and faulted half unit cell, respectively. (c) STS image at the bias voltage of 1.0 V. The inset image indicates the simulated STS curve for dimer structure by DFT. (d) The corresponding amplified image of the area labeled by the blue box in (c). The pair of black dots in (d) represent dimers. (e) and (f) STS images obtained by Pt-Ir (e) and Si-decorated tip (f) with 1.0 V voltage. (g) Line profiles of the STS images along the long diagonal of the unit cell in (e) and (f).

In order to explore dimers, we analyze the PDOSs [Fig. 2(a)] in details. The relative intensity of LDOS of dimers predominates at the energy level about 0.7 eV [green line in Fig. 2(a)], which indicates that the tunneling current around this voltage is mainly contributed from dimers. This deduction is further confirmed by the STS curve [Fig. 4(c)] simulated by DFT calculations for the dimer atoms, which shows a weak peak around 1.0 eV.³¹ The two calculated results consistently suggest an opportunity to observe the dimers by STS image at the bias voltage of ~ 1.0 V. By employment of the p_z -wave tip, STS image of Si (111)- 7×7 surface at 1.0 V bias voltage was carried out as shown in Fig. 4(c). Figure 4(d) is the corresponding magnified image of the area labeled by the blue rectangle in Fig. 4(c). The bright yellow short lines between two hollow dots hint that its information is originated from the tunneling between dimer atoms and Si-decorated tip. As expected, there appear 9 bright short lines in each unit cell, which is consistent with the dimers in the DAS model, as indicated by the pairs of black dots in Fig. 4(d). To further confirm the essential role of p_z tip state for the visualization of the surface states of third-layer dimers, the comparison of STS images at the bias voltage of 1.0 V with Pt-Ir tip and Si-decorated tip was also carried out as shown in Figs. 4(e)–4(g). The strong contrast of STS intensity at the position of dimers [Fig. 4(g)] strongly support the above conclusion, which is well consistent with the previous theoretical work.³⁰ Moreover, one can see that the STS image shows bright pentagons at the three corner of the unfaulted side, as shown in Fig. 4(d). This result is originated from that the LDOS of the unfaulted-half unit cell without dangling bond near the 1.0 eV is higher than that in the faulted-half unit cell, as illustrated in Fig. 2(a).

In summary, we demonstrate that the surface states from the third-layer of Si (111)- 7×7 surface were unprecedentedly uncovered by STS images using Si-decorated tip, which exhibits highly oriented p_z tip state. Apparently, the tip not only determines the lateral resolution of the corrugations, but also the ability to perform reliable spatially resolved

spectroscopy. The Si-modified STM tip with highly directional orbitals compared with that of bare metal tips, may account for the ultra-high resolution image. Hence, the significance of this study goes beyond just the Si (111)- 7×7 case, but also provides opportunities to explore the deep information of other model systems such as MX_2 topological insulators or superconductors with sandwich structures.

See [supplementary material](#) for STM/STS measurements, first principle calculations, tip decoration process and the corrugation amplitude for different tip and sample states.

We gratefully acknowledge the discussions with Dr. Christian R. Ast in Max Planck Institute for Solid State Research. The work at Beijing Normal University is supported by the National Key Research and Development Program of China through Contract 2016YFA0302300. J.Z. also acknowledges the support from “The Fundamental Research Funds for the Central Universities” under Contract 2017EYT26. This work was also supported by China Postdoctoral Science Foundation Funded Project (Grant No. 2018M630153).

¹C. Zhang, G. Chen, K. Wang, H. Yang, T. Su, C. T. Chan, M. M. Loy, and X. Xiao, “Experimental and theoretical investigation of single Cu, Ag, and Au atoms adsorbed on Si(111)-(7 \times 7),” *Phys. Rev. Lett.* **94**(17), 176104 (2005).

²P. Zhang, E. Tevaarwerk, B. N. Park, D. E. Savage, G. K. Celler, I. Knezevic, P. G. Evans, M. A. Eriksson, and M. G. Lagally, “Electronic transport in nanometre-scale silicon-on-insulator membranes,” *Nature* **439**(7077), 703–706 (2006).

³R. Calarco, R. J. Meijers, R. K. Debnath, T. Stoica, E. Sutter, and H. Lüth, “Nucleation and growth of GaN nanowires on Si (111) performed by molecular beam epitaxy,” *Nano Lett.* **7**(8), 2248–2251 (2007).

⁴W. Jin, P.-C. Yeh, N. Zaki, D. Zhang, J. T. Sadowski, A. Al-Mahboob, A. M. van Der Zande, D. A. Chenet, J. I. Dadap, and I. P. Herman, “Direct measurement of the thickness-dependent electronic band structure of MoS₂ using angle-resolved photoemission spectroscopy,” *Phys. Rev. Lett.* **111**(10), 106801 (2013).

⁵X. Wang, Z. Cheng, K. Xu, H. K. Tsang, and J.-B. Xu, “High-responsivity graphene/silicon-heterostructure waveguide photodetectors,” *Nat. Photonics* **7**(11), 888 (2013).

- ⁶K. Majhi, K. Pal, H. Lohani, A. Banerjee, P. Mishra, A. K. Yadav, R. Ganesan, B. R. Sekhar, U. V. Waghmare, and P. S. A. Kumar, "Emergence of a weak topological insulator from the Bi₂Se₃ family," *Appl. Phys. Lett.* **110**(16), 162102 (2017).
- ⁷I. Stich, M. Payne, R. King-Smith, J. Lin, and L. Clarke, "Ab initio total-energy calculations for extremely large systems: Application to the Takayanagi reconstruction of Si (111)," *Phys. Rev. Lett.* **68**(9), 1351 (1992).
- ⁸K. D. Brommer, M. Needels, B. Larson, and J. Joannopoulos, "Ab initio theory of the Si (111)-(7 × 7) surface reconstruction: A challenge for massively parallel computation," *Phys. Rev. Lett.* **68**(9), 1355 (1992).
- ⁹A. L. Koh, K. Bao, I. Khan, W. E. Smith, G. Kothleitner, P. Nordlander, S. A. Maier, and D. W. McComb, "Electron energy-loss spectroscopy (EELS) of surface plasmons in single silver nanoparticles and dimers: influence of beam damage and mapping of dark modes," *ACS Nano* **3**(10), 3015 (2009).
- ¹⁰G. P. Lopinski, D. D. M. Wayner, and R. A. Wolkow, "Self-directed growth of molecular nanostructures on silicon," *Nature* **406**(6791), 48–51 (2000).
- ¹¹Z. Zhu, N. Shima, and M. Tsukada, "Electronic states of Si(100) reconstructed surfaces," *Phys. Rev. B* **40**(17), 11868 (1989).
- ¹²R. Schlier and H. Farnsworth, "Structure and adsorption characteristics of clean surfaces of germanium and silicon," *J. Chem. Phys.* **30**(4), 917–926 (1959).
- ¹³J. Rowe and H. Ibach, "Surface and bulk contributions to ultraviolet photoemission spectra of silicon," *Phys. Rev. Lett.* **32**(8), 421 (1974).
- ¹⁴K. Takayanagi, Y. Tanishiro, M. Takahashi, and S. Takahashi, "Structural analysis of Si (111)-7 × 7 by UHV-transmission electron diffraction and microscopy," *J. Vac. Sci. Technol. A* **3**(3), 1502–1506 (1985).
- ¹⁵B. Voigtländer, *Scanning Probe Microscopy-Atomic Force Microscopy and Scanning Tunneling Microscopy* (Springer, US, 2015), p 194–199.
- ¹⁶Y. L. Wang, H. J. Gao, H. M. Guo, H. W. Liu, I. G. Batyrev, W. E. McMahon, and S. B. Zhang, "Tip size effect on the appearance of a STM image for complex surfaces: Theory versus experiment for Si (111)-(7 × 7)," *Phys. Rev. B* **70**(7), 073312 (2004).
- ¹⁷J. Tersoff and D. R. Hamann, "Theory and application for the scanning tunneling microscope," *Phys. Rev. Lett.* **50**(25), 1998–2001 (1983).
- ¹⁸V. M. Hallmark, S. Chiang, J. F. Rabolt, J. D. Swalen, and R. J. Wilson, "Observation of atomic corrugation on Au(111) by scanning tunneling microscopy," *Phys. Rev. Lett.* **59**(25), 2879 (1987).
- ¹⁹C. J. Chen, "Tunneling matrix elements in three-dimensional space: The derivative rule and the sum rule," *Phys. Rev. B* **42**(14), 8841–8857 (1990).
- ²⁰C. J. Chen, "Microscopic view of scanning tunneling microscopy," *J. Vac. Sci. Technol. A* **9**(1), 44–50 (1991).
- ²¹S. Ohnishi and M. Tsukada, "Molecular orbital theory for the scanning tunneling microscopy," *Solid State Commun.* **71**(5), 391–394 (1989).
- ²²L. Gross, N. Moll, F. Mohn, A. Curioni, G. Meyer, F. Hanke, and M. Persson, "High-resolution molecular orbital imaging using a p-wave STM tip," *Phys. Rev. Lett.* **107**(8), 086101 (2011).
- ²³N. Pavliček, I. Swart, J. Niedenführ, G. Meyer, and J. Repp, "Symmetry dependence of vibration-assisted tunneling," *Phys. Rev. Lett.* **110**(13), 136101 (2013).
- ²⁴P. Sutter, "Energy-filtered scanning tunneling microscopy using a semiconductor tip," *Phys. Rev. Lett.* **90**(16), 166101 (2003).
- ²⁵Y. L. Wang, Z. H. Cheng, Z. T. Deng, H. M. Guo, S. X. Du, and H. J. Gao, "Modifying the STM tip for the "ultimate" imaging of the Si(111)-7 × 7 surface and metal-supported molecules," *Chimia* **66**(1–2), 31–37 (2012).
- ²⁶J. Tersoff and D. Hamann, "Theory of the scanning tunneling microscope," in *Scanning Tunneling Microscopy* (Springer, 1985), pp. 59–67.
- ²⁷J. Mysliveček, A. Stróžecka, J. Steffl, P. Sobotík, I. Ošťádal, and B. Voigtländer, "Structure of the adatom electron band of the Si (111)-7 × 7 surface," *Phys. Rev. B* **73**(16), 161302 (2006).
- ²⁸J. E. Demuth, U. Koehler, and R. J. Hamers, "The STM learning curve and where it may take us," *J. Microsc.* **152**(2), 299–316 (1988).
- ²⁹H. Guo, Y. Wang, and H. Gao, *Scanning Tunneling Microscopy of the Si(111)-7 × 7 Surface and Adsorbed Ge Nanostructures* (Springer, Berlin, Heidelberg, 2009), p. 183–220.
- ³⁰Ó. Paz and J. M. Soler, "Efficient and reliable method for the simulation of scanning tunneling images and spectra with local basis sets," *Phys. Status Solidi* **243**(5), 1080–1094 (2006).
- ³¹M. Smeu, H. Guo, W. Ji, and R. A. Wolkow, "Electronic properties of Si(111)-7 × 7 and related reconstructions: Density functional theory calculations," *Phys. Rev. B* **85**(19), 195315 (2012).